Synthesis, crystal structures, Mössbauer spectra, and redox properties of binuclear and tetranuclear iron-sulfur nitrosyl clusters

N. A. Sanina, I. I. Chuev, S. M. Aldoshin, N. S. Ovanesyan, V. V. Strelets, and Yu. V. Geletii*

Institute of Problems of Chemical Physics, Russian Academy of Sciences, 142432 Chernogolovka, Moscow Region, Russian Federation. Fax: (096) 515 5420. E-mail: sanina@icp.ac.ru

The iron-sulfur nitrosyl complexes $A[Fe_4S_3(NO)_7]$, where $A = Na^+$, NH_4^+, or $N(Bu^n)_4^+$, and $B_2[Fe_2S_2(NO)_4]$, where $B = Na^+$, Cs^+, or $N(Bu^n)_4^+$, were synthesized. Their structures and properties were studied by X-ray diffraction analysis, Mössbauer spectroscopy, and cyclic voltammetry. The effect of the crystal packing on the geometry of the tetranuclear $NH_4[Fe_4S_3(NO)_7]\cdot H_2O$ and binuclear $Cs_2[Fe_2S_2(NO)_4]\cdot 2H_2O$ complexes was analyzed. The changes in the Fe^{57} Mössbauer spectral parameters of the anion in the $B_2[Fe_2S_2(NO)_4]$ series depend on the size of the B cation and agree with variations in the structural parameters of the $Fe[S_2(NO)_2]$ chromophores as well as in the stretching vibrations of the NO groups caused by changes in intermolecular contacts. The presence of electronic states delocalized through the Fe—Fe bonds explains the fact that the electronic states of the $Fe_a(S_2NO)$ and $Fe_b(S_2(NO)_2)$ chromophores in the $[Fe_4S_3(NO)_7]^-$ anion are nearly identical. The binuclear clusters are unstable upon storage in the solid phase and decompose in solutions to form the tetranuclear $[Fe_4S_3(NO)_7]^-$ complexes, sulfur, and nitrogen oxides. The redox properties of the $[Fe_4S_3(NO)_7]^-$ and $[Fe_2S_2(NO_4)]^{2-}$ anions in CH_3CN and THF solutions were studied. The mechanism of reduction of the anion in the tetranuclear cluster is proposed.

Key words: binuclear and tetranuclear clusters, iron-sulfur nitrosyl complexes, X-ray diffraction analysis, Mössbauer spectroscopy, cyclic voltammetry.

The ability of NO to coordinate iron compounds is of great biological importance. The formation of nitrosyl complexes leads to inhibition of hemoproteins, *viz.*, iron-containing enzymes (guanylate cyclase and cytochrome P-450) and hemoglobin, and nonheme iron-containing centers (lipoxygenase, ferritin, and iron-sulfur proteins).[1] It is believed that iron-sulfur proteins are rather long-lived reservoirs of bioactive NO, and NO, which is retained in these reservoirs, can be subsequently used in different nitrosation reactions. It was suggested[2] that in such a manner amines, thiols, and ketones are converted in cells into carcinogenic nitrosoamines, nitrosothiols, and oximes, respectively. Since the NO adducts are extremely unstable, the mechanism of conversions is still poorly understood. Synthetic Fe—S—NO clusters can be used as models of nitrosyl complexes *in vivo*.[3]

In this connection, a search for new stable NO donors based on nitrosyl Fe—S clusters and studies of the relationship between their structures and reactivities are of interest. In spite of the diversity of the known Fe—S nitrosyls, experimental data on their structures are scarce. Thus only the $Cs[Fe_4S_3(NO)_7]$,[4] $(C_6H_5)_4As[Fe_4S_3(NO)_7]$,[5] $((CH_3)_4N)_2[Fe_2S_2(NO)_4]$,[6] and $((Et)_4N)_2[Fe_2S_2(NO)_4]$[7] compounds have been studied.

In this work, a series of Fe—S nitrosyl complexes with the $[Fe_4S_3(NO)_7]^-$ and $[Fe_2S_2(NO)_4]^{2-}$ anions were synthesized and their properties were studied by X-ray diffraction analysis, Mössbauer spectroscopy, and cyclic voltammetry.

Experimental

Sodium and ammonium salts of the cluster heptanitrosotrithiotetraferrate anion (1), $Na[Fe_4S_3(NO)_7]$ (1a) and $NH_4[Fe_4S_3(NO)_7]\cdot H_2O$ (1b), were prepared according to a known procedure[8] by heating an aqueous mixture (200 mL) of iron(II) sulfate (20 g), $NaNO_2$ (8 g), and a 22% aqueous solution of $Na_2S\cdot 9H_2O$ or $(NH_4)_2S$ (5 mL). Ammonium sulfide was prepared according to a procedure reported previously.[9] The sodium salt was filtered off, dried with $CaCl_2$, and recrystallized from anhydrous methanol. The yield was 45%. The ammonium salt was extracted from the reaction mixture with diethyl ether, the solvent was removed, and the complex was dried *in vacuo* and recrystallized from anhydrous methanol. The yield was 23%.

Single crystals of $NH_4[Fe_4S_3(NO)_7]\cdot H_2O$ were prepared by slow crystallization of the complex from a 1 : 1 aqueous-methanolic solution in air at ~20 °C for 48 h. IR: ν(NO) for $Na[Fe_4S_3(NO)_7]$, 1740.2 cm^{-1}; ν(NO) for $NH_4[Fe_4S_3(NO)_7]\cdot H_2O$, 1738.7 cm^{-1}. Found (%): Fe, 39.08; N, 17.25; Na, 4.26; S, 17.48. $NaFe_4S_3N_7O_7$. Calculated (%): Fe, 40.42; N, 17.74; Na, 4.16; S, 17.44. Found (%): H, 1.62;

Translated from *Izvestiya Akademii Nauk. Seriya Khimicheskaya*, No. 3, pp. 443—450, March, 2000.

1066-5285/00/4903-0444 $25.00

Fe, 39.30; N, 19.14; S, 17.00. $Fe_4S_3N_8H_6O_8$. Calculated (%): H, 1.06; Fe, 39.46; N, 19.80; S, 17.02.

Tetrabutylammonium salt $(Bu)_4N[Fe_4S_3(NO)_7]$ (1c) was prepared by mixing $Na[Fe_4S_3(NO)_7]$ (0.72 g) and Bu_4NBr (0.49 g) in water (15 mL). The precipitate of the complex that formed was filtered off, washed several times with water (10-mL portions), dried with $CaCl_2$, and recrystallized from anhydrous methanol. The yield was 55.7%. IR: ν(NO) for $Bu_4N[Fe_4S_3(NO)_7]$, 1725.3 cm^{-1}. Found (%): C, 25.82; H, 4.95; Fe, 27.37; N, 14.04; S, 11.98. $Fe_4S_3C_{16}H_{36}N_8O_7$. Calculated (%): C, 24.88; H, 4.66; Fe, 28.93; N, 14.52; S, 12.40.

Sodium and cesium salts of the cluster tetranitrosodithiodiferrate anion (2), $Na_2[Fe_2S_2(NO)_4]\cdot 4H_2O$ (2a) and $Cs_2[Fe_2S_2(NO)_4]\cdot 2H_2O$ (2b), were synthesized by heating $NH_4[Fe_4S_3(NO)_7]$ (3.12 g) in 10% aqueous solutions of the corresponding alkali (NaOH and CsOH). Iron(III) hydroxide that formed was filtered off. The solvent was removed from the filtrate *in vacuo* over $CaCl_2$. The yields were 48% and 35%, respectively.

Table 1. Principal crystallographic data for single crystals of $NH_4[Fe_4S_3(NO)_7]\cdot H_2O$ (**1b**) and $Cs_2[Fe_2S_2(NO)_4]\cdot 2H_2O$ (**2b**)

Parameter	1b	2b
Weight	M_r = 565.46	M_r = 597.71
System	Triclinic	Monoclinic
Space group	$P\bar{1}$	$P2_1/c$
a/Å	9.451(2)	9.608(2)Å
b/Å	10.00(2)	11.402(2)Å
c/Å	10.577(2)	12.601(3)Å
α/deg	59.02(3)	
β/deg	68.57(3)	107.13(3)
γ/deg	79.05(3)	
V/Å^3	797.9(3)	1319.2(5)
Z	2	4
d/mg m^{-3}	2.353	3.009
Scanning technique	ω/2θ	ω/2θ
Number of reflections	4358	3734
Number of reflections with $[I > 2.0\sigma(I)]$	2632	1196
Refinement based on F	2632	1196
Absorption coefficient, μ/mm^{-1}	2.024	7.968
Crystal dimensions/mm^{-1}	0.5×0.2×0.02	0.3×0.1×0.05
Color of the crystal	Black	Red
R	0.0512	0.0394
S	1.030	1.189
Number of refinable parameters	224	157

Single crystals of $Cs_2[Fe_2S_2(NO)_4]\cdot 2H_2O$ were obtained by removing the solvent from the aqueous solution of the complex over $CaCl_2$ over several days. IR: ν(NO) for $Na_2[Fe_2S_2(NO)_4]\cdot 4H_2O$, 1719.0 cm^{-1}; ν(NO) for $Cs_2[Fe_2S_2(NO)_4]\cdot 2H_2O$, 1676.9 cm^{-1}. Found (%): H, 1.03; Fe, 26.43; N, 12.65; Na, 11.40; S, 15.29. $Na_2Fe_2S_2N_4H_8O_8$. Calculated (%): H, 0.97; Fe, 26.96; N, 13.53; Na, 11.11; S, 15.51. Found (%): H, 0.90; Cs, 53.07; Fe, 21.65; N, 10.50; S, 12.03. $Cs_2Fe_2S_2N_4H_4O_6$. Calculated (%): H, 0.79; Cs, 52.97; Fe, 22.23; N, 11.16; S, 12.83.

Tetrabutylammonium salt $(Bu_4N)_2[Fe_2S_2(NO)_4]$ (2c) was prepared by mixing a solution of $Na_2[Fe_2S_2(NO)_4]\cdot 4H_2O$ (0.51 g) in water (30 mL) and a solution of Bu_4NBr (0.98 g) in water (25 mL). The red precipitate that formed was filtered off under an atmosphere of N_2, washed with a small amount of diethyl ether, and dried on a filter under an inert atmosphere for 6 h and then in a vacuum desiccator over calcined $CaCl_2$. The yield was 65%. IR: ν(NO) for $(Bu_4N)_2[Fe_2S_2(NO)_4]$, 1657.5 cm^{-1}. Found (%): C, 49.36; H, 9.31; Fe, 14.50; N, 10.71; S, 9.47. $Fe_2S_2C_{32}H_{72}N_6O_4$. Calculated (%): C, 49.24; H, 9.23; Fe, 14.31; N, 10.77; S, 8.23.

Elemental analysis for C, H, N, and S was carried out according to a known procedure[10]; Fe and Na were determined by atomic absorption spectroscopy on an AAS-3 spectrophotometer.

The IR spectra were recorded on IKS-29 and Perkin Elmer FTIR-1600 spectrometers in KBr pellets at ~20 °C in air.

X-ray diffraction study. X-ray diffraction data sets for the crystals of the ammonium salt with anion **1** and for the cesium salt with dianion **2** were collected on an automated four-circle KM-4 diffractometer (Mo-Kα radiation). The structures were solved by the direct method using the SHELX-86 program package[11] and refined by the full-matrix least-squares method (SHEXL-93[12]). The hydrogen atoms were revealed from difference Fourier syntheses and only their positional parameters were refined. The principal crystallographic data for single crystals of the ammonium salt with anion **1** and of the cesium salt with anion **2** are given in Table 1. The selected bond lengths and bond angles for these complexes are given in Tables 2 and 3.*

Mössbauer absorption spectra were recorded on a standard Wiss El apparatus (Germany) in the mode of constant acceleration; Co^{57} in a Rh matrix at ~20 °C served as a source. The measurements of the samples at low temperature were performed with the use of a temperature-controlled CF-506 flow-through helium cryostat (Oxford Instruments). The Mössbauer spectra were processed by the least-squares method on the

* The complete tables of the atomic coordinates, the thermal parameters, and the tables of the bond lengths and bond angles were deposited with the Cambridge Structural Database.

Table 2. Selected bond lengths (d) and bond angles (ω) in complex **1b**

Bond	d/Å	Bond	d/Å	Bond	d/Å	Angle	ω/deg
O(32)–N(32)	1.165(9)	Fe(1)–S(1)	2.205(2)	Fe(4)–N(42)	1.661(6)	O(32)–N(32)–Fe(3)	168.0(6)
N(32)–Fe(3)	1.668(6)	Fe(1)–Fe(2)	2.693(2)	Fe(4)–N(41)	1.671(5)	O(31)–N(31)–Fe(3)	171.2(6)
Fe(3)–N(31)	1.675(7)	Fe(1)–Fe(4)	2.701(13)	Fe(4)–S(3)	2.256(2)	O(31)–N(31)–Fe(3)	171.2(6)
Fe(3)–S(2)	2.246(2)	S(1)–Fe(4)	2.264(2)	N(1)–O(1)	1.159(8)	O(1)–N(1)–Fe(1)	176.5(6)
Fe(3)–S(1)	2.257(2)	S(2)–Fe(2)	2.252(2)	N(21)–O(21)	1.168(8)	O(21)–N(21)–Fe(2)	166.4(5)
Fe(3)–Fe(1)	2.697(2)	N(31)–O(31)	1.157(8)	N(22)–O(22)	1.152(7)	O(21)–N(21)–Fe(2)	166.4(5)
Fe(1)–N(1)	1.651(6)	Fe(2)–N(22)	1.669(6)	N(41)–O(41)	1.161(7)	O(22)–N(22)–Fe(2)	166.9(6)
Fe(1)–S(3)	2.205(2)	Fe(2)–N(21)	1.669(6)	N(42)–O(42)	1.157(8)	O(41)–N(41)–Fe(4)	166.9(6)
Fe(1)–S(2)	2.205(2)	Fe(2)–S(3)	2.259(2)			O(42)–N(42)–Fe(4)	169.4(6)

Table 3. Selected bond lengths (d) and bond angles (ω) in complex **2b**

Bond	d/Å	Bond	d/Å	Bond	d/Å	Angle	ω/deg
Cs(1)—O_W(2)	3.165(11)	Cs(2)—O_W(2)	3.211(10)	Fe(1)—S(2)	2.230(4)	N(12)—Fe(1)—N(11)	114.9(6)
Cs(1)—O(12)	3.227(10)	Cs(2)—O(22)	3.244(10)	Fe(1)—S(1)	2.240(4)	N(22)—Fe(2)—N(21)	112.3(6)
Cs(1)—O(11)	3.245(11)	Cs(2)—O(21)	3.322(11)	Fe(1)—Fe(2)	2.703(3)	O(11)—N(11)—Fe(1)	167.9(12)
Cs(1)—O(21)	3.247(11)	Cs(2)—O(11)	3.369(11)	Fe(1)—Cs(1)	3.987(2)	O(21)—N(21)—Fe(2)	166.6(11)
Cs(1)—N(11)	3.352(12)	Cs(2)—O_W(2)	3.454(13)	Fe(1)—Cs(2)	4.190(2)	O(12)—N(12)—Fe(1)	163.8(11)
Cs(1)—S(2)	3.414(4)	Cs(2)—O(12)	3.502(12)	Fe(2)—N(22)	1.654(12)	O(22)—N(22)—Fe(2)	165.4(12)
Cs(1)—S(1)	3.484(4)	Cs(2)—N(21)	3.506(12)	Fe(2)—N(21)	1.665(11)		
Cs(1)—N(21)	3.495(11)	Cs(2)—S(1)	3.572(4)	Fe(2)—S(2)	2.235(4)		
Cs(1)—O_W(2)	3.517(13)	Cs(2)—N(12)	3.574(12)	Fe(2)—S(1)	2.243(4)		
Cs(1)—O(11)	3.568(12)	Cs(2)—N(12)	3.603(11)	O(21)—N(21)	1.155(14)		
Cs(1)—O(22)	3.585(11)	Cs(2)—O(21)	3.719(11)	O(22)—N(22)	1.17(2)		
Cs(1)—N(22)	3.725(13)	Fe(1)—N(12)	1.661(11)	O(11)—N(11)	1.148(14)		
Cs(2)—O_W(1)	3.112(10)	Fe(1)—N(11)	1.675(10)	N(12)—O(12)	1.175(14)		

Note: O_W(1) and O_W(2) are the oxygen atoms of the water molecule of solvation.

assumption that the combined absorption lines take the Lorentz form.

Voltammetric measurements were carried out under a dry inert atmosphere in a THF or MeCN medium, which had been prepurified and distilled directly into an electrochemical cell (evacuated and filled with argon) according to a procedure described previously.[13] Tetrahydrofuran (Aldrich) was purified by the ketyl method. Acetonitrile (Aldrich) was refluxed over P_2O_5 and distilled. A solution of Bu_4NPF_6 was used as the supporting electrolyte. Tetrabutylammonium hexafluorophosphate (Aldrich) was preliminarily dehydrated by melting *in vacuo*. All measured potentials are given relative to an aqueous saturated calomel electrode by comparing the potential of the reference electrode (Ag/AgCl/4 *M* aqueous solution of LiCl), which was separated from the solution studied in the cell by a bridge filled with a solution of the supporting electrolyte, with the potential of the redox transformation of ferrocene$^{0/+}$ (E^0 = 0.44 and 0.42 V, a saturated calomel electrode in THF and MeCN, respectively).

Disk platinum (the diameter was 1 mm) or gold (the diameter was 0.7 mm) electrodes sealed in glass and polished with a diamond paste (the grain size was ≤1 μm) were used as working electrodes. The voltammetric measurements were carried out with the use of a PAR 175 generator of signals and a PAR 173 potentiostat with compensation of ohmic losses. The voltammograms were obtained on a two-coordinate RE0074 automatic recorder.

Results and Discussion

The synthesized nitrosyl complexes with the $[Fe_4S_3(NO)_7]^-$ anion are more stable than complexes with the $[Fe_2S_2(NO)_4]^{2-}$ anion. However, $NH_4[Fe_4S_3(NO)_7]$ partially decomposes to form $Fe(OH)_3$ as one of the decomposition products upon storage in air for one year. The tetranuclear complexes are readily soluble in polar solvents. The binuclear clusters are unstable and require special conditions for storage. Their stability depends on the nature of the cation. Thus the complexes with an organic cation are less stable. For example, compounds with the Na^+ and Cs^+ cations can be stored *in vacuo* for 3—6 months, whereas the compound with the $N(Bu^n)_4^+$ cation can be stored for at most one month. In air, the binuclear complexes are immediately converted into the tetranuclear complexes with the corresponding cation. Sulfur, nitrogen oxides, and unidentified compounds are also among the decomposition products. These complexes are readily soluble and stable in water and acetone (upon storage of solutions under an inert atmosphere) and are insoluble in ether. In polar solvents (methanol or acetonitrile), the binuclear complexes are converted into the tetranuclear complexes.

Anion **1** of the $NH_4[Fe_4S_3(NO)_7] \cdot H_2O$ complex (Fig. 1) exists as a trigonal pyramid whose vertices are occupied by the iron atoms. The ideal symmetry of the anion is described by the C_{3v} group. The distances between the Fe atoms can be characterized by two types of contacts, *viz.*, by contacts between the apical Fe_a atom (Fe(1)) and the Fe_b atoms (Fe(2)—Fe(4)) of the base of the pyramid (Fe(1)—Fe(2), 2.693(1) Å; Fe(1)—Fe(3), 2.696(1) Å; and Fe(1)—Fe(4), 2.707(1) Å) and by contacts between the Fe_b atoms of the base of

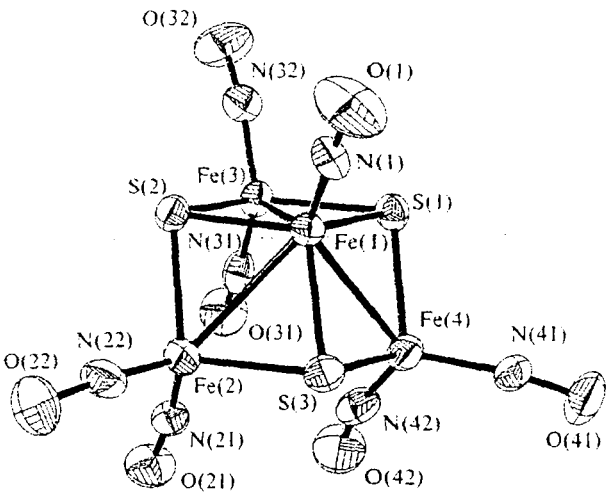

Fig. 1. Overall view of the anion of $NH_4[Fe_4S_3(NO)]_7 \cdot H_2O$ complex (**1b**).

the pyramid (Fe(2)—Fe(3), 3.601(1) Å; Fe(2)—Fe(4), 3.543(1) Å; and Fe(3)—Fe(4), 3.563(1) Å). These data coincide with the values obtained previously for the Cs^+[4] and $AsPh_4^+$[5] salts (Fe_a—Fe_b, 2.700 Å; and Fe_b—Fe_b, 3.570 Å). The Fe_b atoms of the base of the pyramid are linked through the Fe_b—S—Fe_b sulfur bridges, like in the Cs^+ and $AsPh_4^+$ salts studied previously.[4,5] The sulfur atoms of these bridges also form bonds with the apical Fe_a atoms. The average Fe_a—S and Fe_b—S distances (2.205(1) and 2.256(2) Å, respectively) coincide with the published data[4,5] (2.206 and 2.258 Å, respectively). The apical iron atom (Fe_a), *viz.*, Fe(1), is coordinated by one NO ligand and three bridging S atoms, whereas each Fe_b atom (Fe(2), Fe(3), and Fe(4)) is coordinated by two nitrosyl ligands and two bridging S atoms.

Noteworthy are the substantial deviations of two bond lengths (Fe(4)—S(1), 2.264(2) Å; and Fe(3)—S(2), 2.246(2) Å) from the average Fe_b—S bond length. In addition, the planarity of the Fe(1)S(1)Fe(4)S(3) face is somewhat distorted (the folding angle along the Fe(1)—Fe(4) line is 5.0°) compared to the remaining two faces (1.2° and 1.4°).

Analysis of the bond lengths in the nitrosyl ligands demonstrates that the Fe_a—N bond (1.651(2) Å) is shortened compared to the analogous values for the peripheral atoms (Fe_b—N, 1.661(6)—1.675(7) Å). All Fe—N—O fragments are nearly linear. The equatorial angles are 169.4(1), 171.2(1), and 166.4(1)° (*cf.* the literature data[4,5]: 167.5°). The axial angles in complex **1** are 166.9(1), 166.9(1), and 168.0(1)° (*cf.* the literature data[4,5]: 166.1°), *i.e.*, these angles are larger than the Fe_a—N—O angle (176.5(1)°; *cf.* the literature data[4,5]: 176.3°).

Apparently, the differences in these angles are caused by the formation of intermolecular hydrogen bonds NH_4^+...ON ($N(NH_4^+)$...O(21), 3.10 Å; and $N(NH_4^+)$...O(21′), 3.15 Å) and H_2O...ON ($O(H_2O)$...O(21), 2.99 Å; $O(H_2O)$...O(21′), 3.11 Å; and $O(H_2O)$...O(41), 3.10 Å). The increase in the N(31)—Fe(3)—N(32) bond angle (119.1(1)°) compared to the remaining two angles (N(21)—Fe(2)—N(22), 115.6(1)°; and N(41)—Fe(4)—N(42), 115.7(1)°) is also of interest. Evidently, this change in the geometry is governed by the formation of a chain of intermolecular hydrogen bonds NH_4^+...O(32) (N...O, 3.25 Å) and NH_4^+...O(31) (N...O, 3.15 Å), which "extend" the nitrosyl ligands at the Fe(3) atom resulting in the observed increase in the angle.

Dianion **2b** in the cesium complex (Fig. 2), as in the salts with the $(CH_3)_4N^+$[6] and $(Et)_4N^+$[7] cations studied previously, has the approximate symmetry D_{2h}. Two Fe atoms are linked through two bridging S atoms. Therefore, the bridging S atoms in complex **2**, unlike those in complex **1**, form bonds with only two rather than with three Fe atoms. The Fe atoms are coordinated by two bridging S atoms and two NO ligands. The Fe—N—O fragments, like those in **1**, are linear. The Fe—N—O

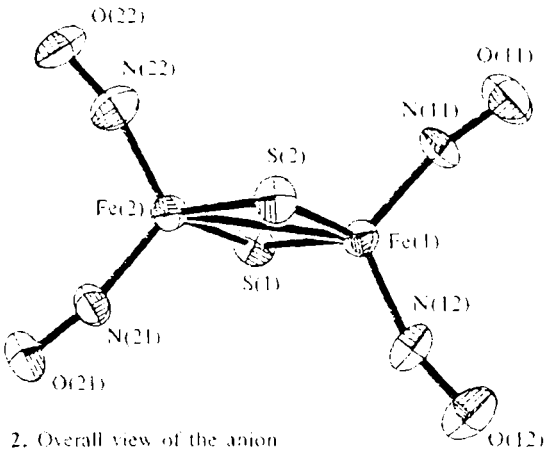

Fig. 2. Overall view of the anion of the $Cs_2[Fe_2S_2(NO)_4]\cdot 2H_2O$ complex (**2b**)

angles are in the range of 164(1)—168(1)°, which coincides with the range for the Fe_b—N—O values in anion **1b**.

Noteworthy is the decrease in the size of dianion **2** compared to the dianion in the salts with the Me_4N^+ and Et_4N^+ cations.[6,7] The Fe—S bond lengths in dianion **2** are in the range of 2.232(3)—2.243(2) Å (2.239—2.250 Å for the anion in the salt with the Me_4N^+ cation; 2.239 and 2.241 Å for the anion in the salt with the Et_4N^+ cation); the Fe—Fe bond length in dianion **2** is 2.702(2) Å (2.713 and 2.716, and 2.713 Å, for the anions in the salts with the Me_4N^+ and Et_4N^+ cations, respectively). This may be associated with the smaller size of the Cs^+ cation in the complex with dianion **2** compared to Me_4N^+ and Et_4N^+, as a result of which the degree of transfer of the electron density from the highest occupied molecular orbital of the anion to the cation in the complex with dianion **2** is decreased. Since this orbital is bonding[18] and consists predominantly of the d orbitals of the Fe_4 core, this geometric behavior of the anion can be adequately described within the framework of the Hückel theory (EHMO).

Noteworthy also is the substantial difference in the N(11)—Fe(1)—N(12) and N(21)—Fe(2)—N(22) bond angles (114.7(4)° and 112.7(4)°, respectively), which apparently results from the nonequivalence of the crystal environment. Analysis of the intermolecular Cs...N contacts shows that the environment about the N(11) atom (Cs(1)...N(11), 3.351 Å) is substantially different from those about the remaining nitrogen atoms (Cs...N, 3.49—3.77 Å). For the intermolecular Cs...O contacts, two pairs of nitrosyl ligands with an approximately equivalent crystal environment can be distinguished.

Analysis of the crystal packing demonstrates that the coordination number of Cs^+ is 12 and the Cs^+...ligand distances are in the ranges of 3.165(11)—3.725(13) and 3.112(10)—3.719(11) Å for the Cs(1) and Cs(2) atoms, respectively. However, analysis of the Cs...Cs contacts shows that these distances in the crystal are smaller than

Table 4. Parameters of the Mössbauer spectra of the binuclear and tetranuclear complexes obtained at 78 K

Complex	Coordination about the Fe atom	δ_{Fe}[a]	ΔE_Q[b]	Γ[c]	Intensity
		mm s^{-1}			
$(NH_4)[Fe_4(\mu_3\text{-}S)_3(NO)_7]\cdot H_2O$ (**1a**)	$\{S_2(NO)_2\}$	0.154	0.957	0.28	3
	$\{S_3(NO)\}$	0.158	0.733	0.24	1
$(Bu^n_4N)[Fe_4(\mu_3\text{-}S)_3(NO)_7]$ (**1b**)	$\{S_2(NO)_2\}$	0.141	0.894	0.30	3
	$\{S_3(NO)\}$	0.166	0.635	0.29	1
$Na_2[Fe_2(\mu_2\text{-}S)_2(NO)_4]\cdot 4H_2O$ (**2a**)	$\{S_2(NO)_2\}$	0.091	0.510	0.28	1
	$\{S_2(NO)_2\}$	0.104	0.827	0.28	1
$Cs_2[Fe_2(\mu_2\text{-}S)_2(NO)_4]\cdot 2H_2O$ (**2b**)	$\{S_2(NO)_2\}$	0.078	0.368	0.27	–
$(Bu^n_4N)_2[Fe_2(\mu_2\text{-}S)_2(NO)_4]$ (**2c**)	$\{S_2(NO)_2\}$	0.064	0.258	0.27	–
$Fe_4(\mu_3\text{-}S)_4(NO)_4$[d]	$\{S_3(NO)\}$	0.150	1.473	0.334	–

[a] δ_{Fe} is the isomeric shift relative to Fe at 78 K.
[b] ΔE_Q is the quadrupole splitting.
[c] Γ is the line width.
[d] Literature data.[14]

the metal–metal bond length (Cs(1)—Cs(1), 4.285 Å; Cs(2)—Cs(1), 4.738 and 5.664 Å; and Cs(2)—Cs(2), 4.832 Å). Apparently, the positive charge in the crystal is only partially localized on the Cs atoms; otherwise these Cs...Cs contacts in the crystal cannot occur.

With the aim of obtaining additional data on the structures of the iron-sulfur nitrosyl clusters, we studied a series of complex salts with different cations, including compounds for which data on the molecular and crystal structures are unavailable, by Mössbauer spectroscopy.

The parameters of the ^{57}Fe Mössbauer spectra of a series of $A_2[Fe_2S_2(NO)_4]$ binuclear complexes, where A = Na^+, Cs^+, or Bu_4N^+, and $A[Fe_4S_3(NO)_7]$ tetranuclear complexes, where A = NH_4^+ or $Bu^n_4N^+$, at 78 K are given in Table 4. In this table, the data for the neutral cubane-like tetramer $[Fe_4S_4(NO)_4]$[14] are given for comparison.

The Mössbauer spectrum of the sodium salt of the binuclear complex with dianion **2** is adequately described as a superposition of two symmetrical quadrupole doublets (Fig. 3, *a*). Their intensity ratio is 1 : 1, provided that the line widths of the individual doublets are equal. This result is most likely indicative of the structural nonequivalence of the iron positions in the dimer in spite of the identical composition of the coordination environment, $(\mu_2\text{-}S)_2(NO)_2$. On the contrary, the spectra of the binuclear complexes with the cesium or tetrabutylammonium cations or with dianion **2** (Fig. 3, *b*, *c*) are adequately described by one asymmetrical doublet with insignificantly broadened lines (see Table 4) in spite of the revealed structural nonequivalence of the Fe atoms in the dimer of the cesium salt. The asymmetry of the absorption lines in spectra *b* and *c* (Fig. 3) is associated with the pro-

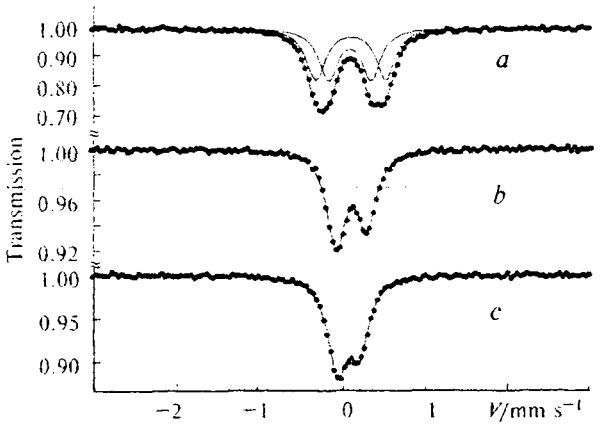

Fig. 3. Mössbauer spectra of the binuclear complexes with the $[Fe_2S_2(NO_4)]^{2-}$ dianion (**2**) and with the Na^+ (*a*), Cs^+ (*b*), and $(Bu^n_4N)^+$ (*c*) cations (78 K).

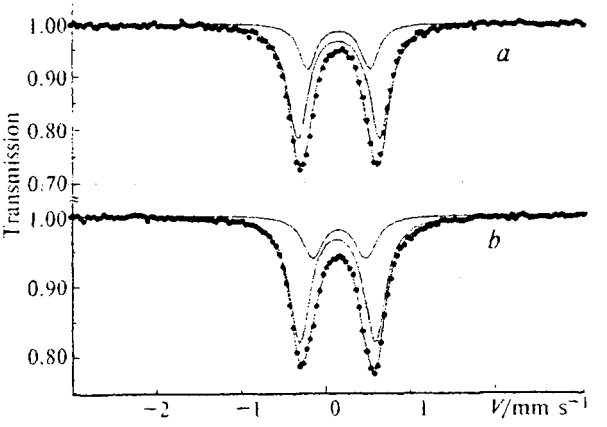

Fig. 4. Mössbauer spectra of the tetranuclear complexes with the $[Fe_4S_3(NO_7)]^-$ anion (**1**) and with the NH_4^+ (*a*) and $(Bu^n_4N)^+$ (*b*) cations (78 K).

nounced texture of the samples, which comprise sets of needle-like single crystals of different lengths. Their axes are located predominantly in the plane perpendicular to the direction of the γ-quantum beam.

The spectra of the samples of the tetramers with anion **1** of the ammonium (*a*) and tetrabutylammonium salts (*b*) were processed as superpositions of two doublets with the fixed ratio of integrated intensities of 3 : 1 (Fig. 4). This ratio corresponds to the relative weights of two structurally nonequivalent positions of the iron atoms, *viz.*, Fe_b and Fe_a, in the $[Fe_4(NO)_7S_3]^-$ anion, which differ in the formal charge and in the composition of the coordination sphere. Note that the parameters of the Mössbauer spectra of the complex with the ammonium cation and anion **1**, which were obtained in the early studies[14,15] at the same ratio (3 : 1) of the relative contributions of the Fe_b and Fe_a states, are substantially different (particularly, in the isomeric shift for Fe_a; δ_a is 0.25 mm·s^{-1}). Since the spectral resolution was inadequate, it was rather difficult to unambiguously choose a particular set of parameters. Nevertheless, the spectral parameters of the $NH_4[Fe_4S_3(NO)_7]$ and $Bu^n_4N[Fe_4S_3(NO)_7]$ compounds given in Table 4 correspond to the lower (by ~20%) value of the χ^2 parameter compared to the alternative set of parameters similar to those obtained previously.[14,15] In addition, it can be seen from Table 4 that in the case of the chosen set of parameters, the values of the isomeric shift δ for Fe_a fall in the range of the δ shifts for the equivalent Fe^{2+} states in the neutral $[Fe_4S_4(NO)_4]$ complex[14] with the identical composition of the coordination environment.

Judging from the noticeable dependence of the ^{57}Fe Mössbauer spectral parameters (see Table 4) on the type of the cation in the crystals under study, the role of the cation is not limited to the simple compensation of the negative charge of the cluster. The cation also noticeably affects the structure of the cluster, *i.e.*, the angles and interatomic bond lengths. The above-mentioned effect is most pronounced in the series of crystals of the binuclear complexes with dianion **2**.

The dependences of the changes in the Mössbauer spectral parameters, the isomeric shift (δ), and the quadrupole splitting (ΔE_Q) on the size of counter-ion A are of interest. Thus the ΔE_Q value decreases substantially as the size of ion A increases (on the average, from 0.70 for A = Na^+ to 0.26 mm·s^{-1} for A = $Bu^n_4N^+$), *i.e.*, the total distribution of the charges of the valence shells of the Fe atom and of the atoms surrounding the iron atom is more symmetrical. This fact is surprising when taking into account the difference in the composition of the nearest ligand environment about the iron atoms, $(\mu_2\text{-}S)_2(NO)_2$, and evidently the substantial difference in the effective charges of the sulfur atoms and the nitrosyl groups. The formal charge on the Fe atom is −1, which corresponds to the d^9 electronic configuration and to the expected substantial contribution of this configuration to ΔE_Q. Apparently, the small value of ΔE_Q for A = Bu_4N^+ and its independence from the temperature indicate that the contributions of the charges of the surrounding atoms and the charge of the d shell of the iron atom to ΔE_Q are almost completely compensated.

It is also worthy of note that the isomeric shift δ substantially decreases as the size of cation A increases (see Table 4). This behavior indicates that the s electron density on the Fe^{57} nuclei increases on going from A = Na^+ to Bu_4N^+, which may be a result of a decrease in the Fe—S and Fe—Fe bond lengths. The tendency for a decrease in the lengths of the above-mentioned bonds has been observed previously on going from the Me_4N^+ salt to the Cs^+ salt and it has been attributed to an increase in the degree of localization of the electron density on the bonding (relative to the Fe—Fe bonds) highest occupied molecular orbital of the dianion. Apparently, Me_4N^+ is more electrophilic than Cs^+ due to superconjugation. In turn, a decrease in the occupancy of the lowest unoccupied MO of the dianion, which consists primarily of the d orbitals of the Fe atom,[19] should favor a decrease in the dπ(Fe)→π*(NO) back donation and, correspondingly, should lead to strengthening of the N—O bond.[20] This situation is confirmed by the fact that the average stretching fre-

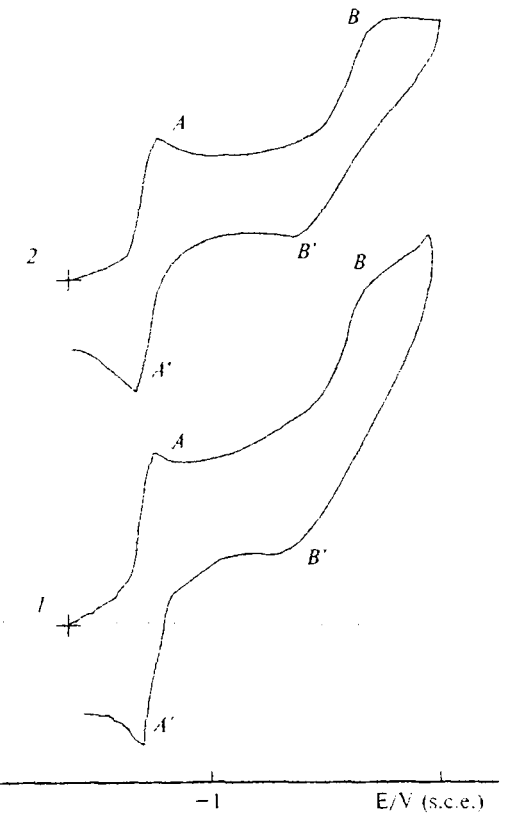

Fig. 5. Cyclic voltammograms of the complexes with anions **1** (curve *1*, 4.2·10^{-3} mol L^{-1}) and **2** (curve *2*, 7.1·10^{-3} mol L^{-1}) in a THF/0.1 *M* Bu_4NPF_6 medium on a Pt electrode (v = 0.2 V/s) at 20±2 °C.

quencies of the NO groups in the IR spectra of the Cs^+ and $Bu^n_4N^+$ salts are 42.1 and 62 cm^{-1} lower, respectively, than the value observed for the sodium salt (1719.0 cm^{-1}).

The electrochemical behavior of the tetrabutylammonium complexes with anions **1** and **2** was studied by cyclic voltammetry. The cyclic voltammograms of the cluster with anion **1** in MeCN/0.05 *M* Bu_4NPF_6 and THF/0.1 *M* Bu_4NPF_6 media have two peaks (*A* and *B*). A typical voltammogram in MeCN is shown in Fig. 5 (curve *1*). All observed peaks are diffusion-controlled ($I_p \cdot v^{-1/2}$ = const, where I_p is the peak height and v is the rate of the linear potential scan) and one-electron, which is evident from a comparison of their heights with the height of the one-electron reduction peak of the $HRu_4(CO)_{12}$ cluster determined under identical conditions.[16] The choice of $HRu_4(CO)_{12}$ instead of ferrocene as the standard was governed by more similar sizes and, consequently, by the closer values of the diffusion coefficients of this compound and the complex with anion **1**. In a MeCN medium at potentials more positive than +0.7 V (saturated calomel electrode (s.c.e.)), the cluster with anion **1** underwent irreversible multielectron oxidation accompanied, most likely, by destruction of the structure of the complex (reduction waves were also observed).

At the first stage, reduction of the salt with anion **1**, unlike irreversible oxidation, is reversible as evidenced by the value $\Delta E_p = E_p^a - E_p^c = 70$ mV (E_p^c and E_p^a are the potentials of the cathodic and anodic peaks, respectively) and by the equality of the heights of the cathodic and anodic responses *A* and *A'* in MeCN. At the second stage, reduction is quasireversible or irreversible ($\Delta E_p \approx$ 300–400 mV). The ΔE_p value for the redox pair *A*/*A'* in a THF medium is somewhat larger (150 mV) due to the larger ohmic resistance in this solvent because the ΔE_p value for the known reversible ferrocene$^{0/+}$ redox pair in THF is 150 mV. The formal standard potentials ($E^0 = (E_p^c + E_p^a)/2$) for the redox pair *A*/*A'* and the potentials of cathodic peak *B* in MeCN and THF media are given in Table 5.

Table 5. Potentials of reduction peaks of the clusters with anions **1** and **2** (relative to a saturated calomel electrode) in MeCN/0.05 *M* Bu_4NPF_6 (Au electrode) and THF/0.1 *M* Bu_4NPF_6 (Pt electrode) at $v = 0.2$ V s^{-1} and $T = 20\pm2$ °C

Cluster with the anion	Peak	E^0 (E_p^c)	
		MeCN	THF
1	*A*/*A'*	−0.72	−0.93
	B	(−1.68)	(−1.74)
	B''	(−1.32)	(−1.44)
2	*A*/*A'*	−0.72	−0.94
	B	(−1.72)	(−1.69)
	B''	(−1.30)	(−1.43)

A slight difference in the reduction potentials of the cluster with anion **1** in THF and MeCN solutions is attributable to the difference in the donor-acceptor properties of these solvents. The data of cyclic voltammetry for complex **2** are given in Fig. 5 (curve *2*). It can be seen that the voltammograms of the tetrabutylammonium complexes with anions **1** and **2** are virtually identical both in shape and potentials of the peaks (see Table 5). Thus in solvents containing donor molecules, the dianion immediately decomposes followed by the formation of the tetranuclear $[Fe_4S_3(NO)_7]^-$ complex. This is evidenced by the data of cyclic voltammetry of the binuclear complex (see Fig. 5) as well as by the IR spectra of powders of these compounds prepared by recrystallization from MeCN (Fig. 6). An analogous situation was also observed upon recrystallization of these compounds from THF. Note that, according to the data reported previously,[17] the cluster with anion **2** in a CH_2Cl_2 medium was also converted into the cluster with anion **1**. Apparently, this reflects the general tendency of the binuclear complex with anion **2** to undergo conversions in solutions to form the thermodynamically more stable tetranuclear cluster with anion **1**. The binuclear complex, in turn, exists predominantly in basic media. For this reason, attempts to prepare and isolate products of one-electron reduction or oxidation of the $[Fe_2S_2(NO)_4]^{2-}$ dimer failed.

Therefore, it can be concluded that the structure of the $[Fe_2S_2(NO)_4]^{2-}$ dianion in the salts of binuclear complexes containing bulky ammonium cations (B = $Bu^n_4N^+$) is least disturbed by intermolecular cation–anion contacts and, apparently, more adequately corresponds to the notion of the structures of the isolated molecules.

A substantial difference in the size of the NH^{4+} and $Bu^n_4N^+$ cations in the tetranuclear complexes with anion **1** affects the parameters of the Mössbauer spectra of the Fe_a and Fe_b states to a lesser extent compared to the observed changes in the series of the binuclear complexes with anion **2**. The lack of structural data on the $Bu^n_4N^+$ salt with the $[Fe_4S_3(NO)_7]^-$ monoanion does

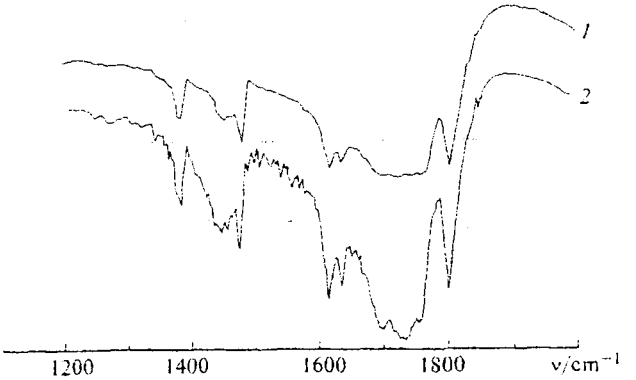

Fig. 6. IR spectra of the binuclear ($(Bu^n_4N)_2[Fe_2S_2(NO)_4]$) (*1*) and tetranuclear ($Bu^n_4N[Fe_4S_3(NO)_7]$) (*2*) complexes recrystallized from MeCN.

not allow one to establish a correlation between the changes in the structural and Mössbauer parameters of the salts under study (due, particularly, to the fact that the isomeric shifts for the Fe_a and Fe_b positions have close values in spite of a substantial difference in their coordination environment). A detailed analysis of the local environments about the Fe_a and Fe_b atoms makes it possible to qualitatively explain the apparent anomaly. Thus the expected increase in the δ_b value in the case of the larger number of d electrons at the $Fe_b(d^9)$ center compared to that at the $Fe_a(d^7)$ center is, apparently, compensated by a decrease in the δ_b value due to the presence of an additional π-acceptor NO^+ group involved in the environment about the Fe_b atoms and the smaller numbers of the Fe—S and Fe—Fe bonds about Fe_b. According to the results of quantum-chemical calculations,[18] the lowest unoccupied MO of the cluster with anion **1** (to which the orbitals of the Fe—Fe bond make the major contribution) is antibonding. Nevertheless, one-electron reduction of anion **1** is reversible. This indicates that the $[Fe_4S_3(NO)_7]^{\cdot 2-}$ dianion radical is stable at least within the time scale of cyclic voltammetry. The total two-electron reduction of anion **1** is irreversible. This indicates that the transfer of the second electron to the cluster causes substantial structural changes resulting, apparently, in destruction of its core. Therefore, the results obtained make it possible to represent the mechanism of reduction of anion **1** by the following scheme:

$$[Fe_4S_3(NO)_7]^- + e \rightleftharpoons$$
$$\rightleftharpoons [Fe_4S_3(NO)_7]^{\cdot 2-} + e \longrightarrow$$
$$\longrightarrow [Fe_4S_3(NO)_7]^{3-} \longrightarrow \text{products.}$$

To summarize the results of the structural and Mössbauer investigations and the data on the redox properties of the resulting compounds, one can conclude that the $[Fe_2S_2(NO)_4]^{2-}$ dianion is more "labile" and its geometry, *i.e.*, the interatomic distances and angles, in the crystal depends more noticeably on the type of the counter ion compared to the $[Fe_4S_3(NO)_7]^-$ monoanion, which is less susceptible to the influence of changes in the intermolecular bonds.

This work was financially supported by the International Association for the Promotion of Cooperation with the Scientists from the New Independent States of the Former Soviet Union (INTAS, Grant 93-1060) and by the Russian Foundation for Basic Research (Project No. 99-03-32484).

References

1. J. W. Raebiger, Ch. A. Crawford, J. Zhou, and R. H. Holm, *Inorg. Chem.*, 1997, **36**, 994.
2. M. Fontecave and J.-L. Pierre, *Bull. Soc. Chim. Fr.*, 1994, **131**, 620.
3. J. Zhou, J. W. Raebiger, and Ch. A. Crawford, *J. Am. Chem. Soc.*, 1997, **119**, 6242.
4. G. Johansson and W. N. Lipscomb, *Acta Crystallogr.*, 1958, **11**, 594.
5. C. T.-W. Chu and L. F. Dahl, *Inorg. Chem.*, 1977, **16**, 3245.
6. X. Lin, A. Zheng, Sh. Lin, J. Huang, and J. Lu, *J. Struct. Chem. (Wuhan)*, 1982, **1**, 79.
7. L. Huang, X. Zhao, B. Zhuang, and H. Jiegon, *J. Struct. Chem. (Wuhan)*, 1992, **11**, 397.
8. Yu. V. Karyakin and I. I. Angelov, *Chistye khimicheskie veshchestva* [*Pure Chemical Compounds*], Khimiya, Moscow, 1974, 42 (in Russian).
9. *Handbuch der Praparativen Anorganischen Chemie*, G. Brauer, Enke, Stuttgart, 1960, **2**, 1526.
10. V. A. Klimova, *Osnovnye mikrometody analiza organicheskikh soedinenii* [*Principal Micromethods of Analysis of Organic Compounds*], Khimiya, Moscow, 1975, 21 (in Russian).
11. J. M. Sheldrick, SHELX-86, Program for the solution of crystal structure, University of Göttingen, Germany, 1985.
12. J. M. Sheldrick, SHELXL-93, Program for the refinement of crystal structure, University of Göttingen, Germany, 1993.
13. V. V. Strelets and K. J. Pikket, *Elektrokhimiya*, 1994, **30**, 1023 [*Russ. J. Electrochem.*, 1994, **30** (Engl. Transl.)].
14. E. Kostiner, J. Steger, and J. R. Rea, *Inorg. Chem.*, 1970, **9**, 1939.
15. C. T.-W. Chu, F. Y. K. Lo, and L. F. Dahl, *J. Am. Chem. Soc.*, 1982, **104**, 3409.
16. D. Osella, C. Nervi, M. Ravera, J. Fidler, and V. V. Strelets, *Organometallics*, 1995, **14**, 2501.
17. S. S. Sung, C. Glidewell, A. R. Butler, and R. Hoffmann, *Inorg. Chem.*, 1985, **24**, 3856A.
18. R. Butler, C. Glidewell, and M.-H. Li, *Adv. Inorg. Chem.*, 1988, **32**, 335.
19. C. T.-W. Chu, F. Y. K. Lo, and L. F. Dahl, *J. Am. Chem. Soc.*, 1982, **104**, 3409.
20. A. R. Butler, C. Glidewell, A. R. Hyde, and J. McGinnis, *Inorg. Chem.*, 1985, **24**, 2931.

Received February 22, 1999;
in revised form September 22, 1999